

Medical Nuclear Supply Chain Design: A Tractable Network Model and Computational Approach

Anna Nagurney¹ and Ladimer S. Nagurney²

¹John F. Smith Memorial Professor - Isenberg School of Management
University of Massachusetts - Amherst, Massachusetts 01003

²Department of Electrical and Computer Engineering
University of Hartford - West Hartford, CT 06117

58th Annual North American Meetings of the Regional Science
Association International
Miami, Florida
November 9-12, 2011

Outline

- ▶ Background and Motivation
- ▶ Supply Chain Challenges
- ▶ The Medical Nuclear Supply Chain Network Design Model
- ▶ The Computational Approach
- ▶ Highlights of a Case Study
- ▶ Summary and Suggestions for Future Research

This presentation is based on the paper, “Medical Nuclear Supply Chain Design: A Tractable Network Model and Computational Approach,” by A. Nagurney and L. S. Nagurney, where a full list of references can be found.

Background and Motivation

Medical Nuclear Supply Chains

Medical nuclear supply chains are essential supply chains in healthcare and provide the conduits for products used in nuclear medical imaging, which is routinely utilized by physicians for diagnostic analysis for both cancer and cardiac problems.

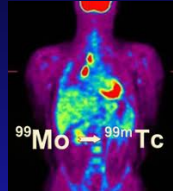
Such supply chains have unique features and characteristics due to the products' time-sensitivity, along with their hazardous nature.

Salient Features:

- ▶ complexity
- ▶ economic aspects
- ▶ underlying physics of radioactive decay
- ▶ importance of considering waste management.

Nuclear Medicine

To create an image for medical diagnostic purposes, a radioactive isotope is bound to a pharmaceutical that is injected into the patient and travels to the site or organ of interest.



The gamma rays emitted by the radioactive decay of the isotope are then used to create an image of that site or organ.

Technetium, $^{99\text{m}}\text{Tc}$, which is a decay product of Molybdenum, ^{99}Mo , is the most commonly used medical radioisotope, accounting for over 80% of the radioisotope injections and representing over 30 million procedures worldwide each year.

Nuclear Medicine

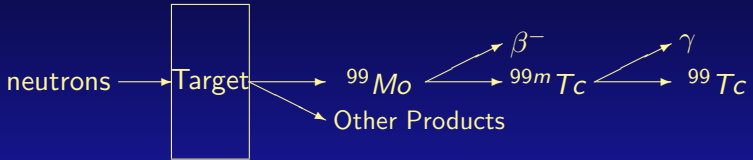
Over 100,000 hospitals in the world use radioisotopes (World Nuclear Association (2011)).

In 2008, over 18.5 million doses of ^{99m}Tc were injected in the US with 2/3 of them used for cardiac exams

It is estimated that the global market for medical isotopes is 3.7 billion US\$ per year (Kahn (2008)).

Nuclear Physics Background

To create ^{99m}Tc , an enriched Uranium target is irradiated with neutrons in a reactor. After irradiation, the ^{99}Mo product is separated from the other products and purified.



The ^{99}Mo decays by emitting a β^- to create ^{99m}Tc with a $t_{1/2}$ of 66.7 hours.

The ^{99m}Tc decays by emitting a γ to create ^{99}Tc with a $t_{1/2}$ of 6 hours.

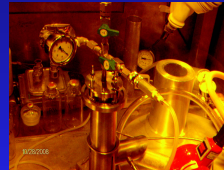
It is the γ emitted from the ^{99m}Tc decay that creates the image.

Nuclear Physics Background

The irradiated targets are highly radioactive and must be handled and shipped with extreme caution. The only shipping method that is allowed is via truck.



At the processing plant the ^{99}Mo is separated and purified.

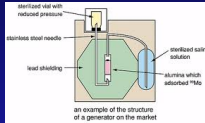


The purified Mo is shipped to generator manufacturers, where it is packaged in generators, which are then shipped to hospitals and medical imaging facilities worldwide. *Multiple modes of transportation can be used at this stage.*



^{99m}Tc Generators

Inside a generator, the ^{99}Mo and the ^{99m}Tc are in an ion column. A saline solution is used to elute the ^{99m}Tc , which is then prepared for injection into the patient.



The Production of ^{99}Mo

The production of ^{99}Mo occurs at only nine reactors in the world.

Reactor name	Location	Annual operating days	Normal production per week ^a	Weekly % of world demand	Fuel/targets ^b	Date of first commissioning
BR-2	Belgium	140	5 200 ^c	25-65	HEU/HEU	1961
HFR	Netherlands	300	4 680	35-70	LEU/HEU	1961
LVR-15 ^d	Czech Rep.	–	>600	–	HEU ^e /HEU	1957
MARIA ^d	Poland	–	700-1 500	–	HEU/HEU	1974
NRU	Canada	300	4 680	35-70	LEU/HEU	1957
OPAL	Australia	290	1 000-1 500	– ^f	LEU/LEU	2007
OSIRIS	France	180	1 200	10-20	LEU/HEU	1966
SAFARI-1	South Africa	305	2 500	10-30	LEU/HEU ^g	1965
RA-3	Argentina	230	200	< 2	LEU/LEU	1967

Source: The Supply of Medical Radioisotopes: An Economic Study of the Molybdenum-99 Supply Chain, OECD (2010)

Production of ^{99}Mo - $^{99\text{m}}\text{Tc}$ for the US



Supply Chain Challenges

Supply Chain Challenges

With a 5% annual growth rate for imaging, the demand will exceed the supply by the end of the decade.

This assumes that all reactors are capable of irradiating the targets at all times.

With routine maintenance, unexpected maintenance, and shutdowns due to safety concerns, there have been severe disruptions over the past several years.

In 2009, the demand exceeded the supply and created a worldwide shortage of ^{99}Mo .

Supply Chain Challenges

Several of the reactors are reaching the end of their lifetimes, since they are 40 to over 50 years old.

Between 2000 and 2010, there were six unexpected shutdowns of reactors used for medical imaging products due to safety concerns with the Canadian one shut down in May 2009 due to a leak in the reactor with its return to service more than a year later in August 2010.

There are only four bulk ^{99}Mo processors that supply the global market, located in: Canada, Belgium, The Netherlands, and South Africa.

Australia and Argentina produce bulk ^{99}Mo for their domestic markets but are expected to export small amounts in the future.

Supply Chain Challenges

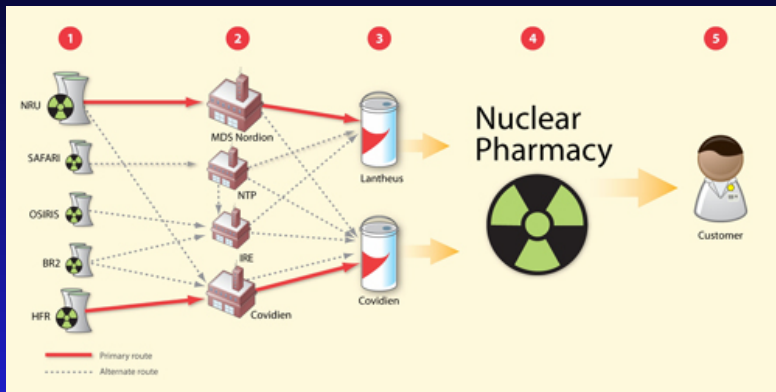
There are parts of the world in which there are no processing facilities for ^{99}Mo , including the United States, parts of South America, and Japan.

Such limitations in processing capabilities limit the ability to produce the medical radioisotopes from regional reactors since long-distance transportation of the *Mo* targets raises safety and security risks, and also results in greater decay of the product.

The number of generator manufacturers with substantial processing capabilities is under a dozen.

In 2015, the Canadian reactor is scheduled for complete shutdown, raising critical questions for supply chain network redesign, since its processing facility will also need to be shut down.

^{99}Mo Supply Chain for the US



The Medical Nuclear Supply Chain Network Design Model

The Medical Nuclear Supply Chain Network Design Model

We consider a possible network topology of the medical nuclear supply chain. We assume that, in the initial supply chain network topology, as in Figure 1, which serves as a template upon which the optimal supply chain network design is constructed, there exists at least one path joining node 0 with each destination node: $H_1^2, \dots, H_{n_H}^2$. This assumption guarantees that the demand at each demand point will be met.

The initial template should include both existing facilities (nodes) and processes (links) as well as prospective new ones that are to be quantifiably evaluated and selected from.

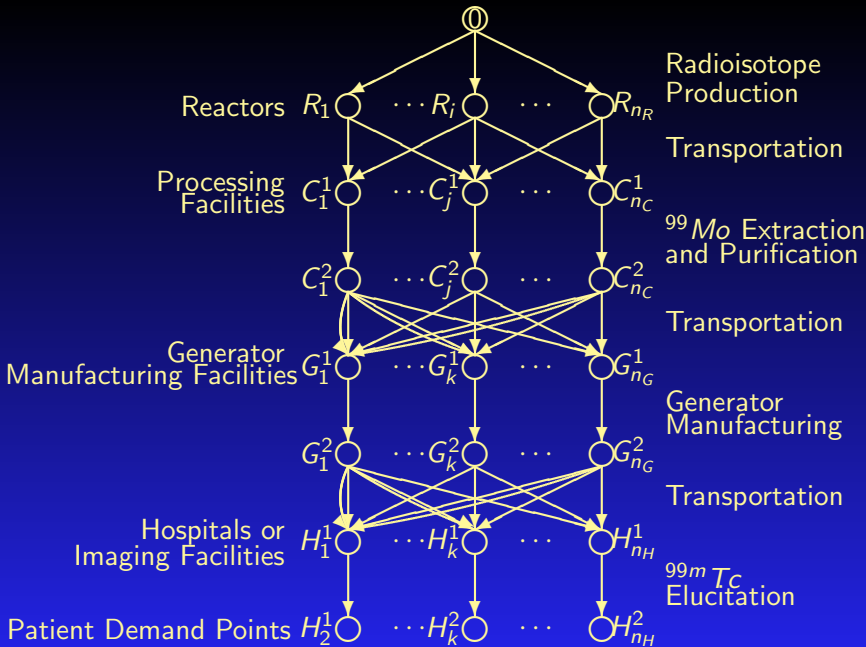


Figure 1: The Medical Nuclear Supply Chain Network Topology

The possible supply chain network topology, as depicted in Figure 1, is represented by $\mathcal{G} = [N, L]$, where N and L denote the sets of nodes and links, respectively. The ultimate solution of the complete model will yield the optimal capacity modifications on the various links of the network as well as the optimal flows.

Let w_k denote the pair of origin/destination (O/D) nodes $(0, H_k^2)$ and let \mathcal{P}_{w_k} denote the set of paths, which represent the alternative associated possible supply chain network processes, joining $(0, H_k^2)$. \mathcal{P} denotes the set of all paths joining node 0 to the destination nodes, and $n_{\mathcal{P}}$ denotes the number of paths.

Let d_k denote the demand for the radioisotope at the demand point H_k^2 ; $k = 1, \dots, n_H$.

The Link Operational Costs

With each link of the network, we associate a unit operational cost function that reflects the cost of operating the particular supply chain activity. The links are denoted by a, b , etc.

The unit operational cost on link a is denoted by c_a and is a function of flow on that link, f_a . The *total* operational cost on link a is denoted by \hat{c}_a , and is constructed as:

$$\hat{c}_a(f_a) = f_a \times c_a(f_a), \quad \forall a \in L. \quad (1)$$

The link total cost functions are assumed to be convex and continuously differentiable.

Capturing the Underlying Physics Through Link and Path Multipliers

We associate with every link a in the network, a multiplier α_a , which corresponds to the percentage of decay and additional loss over that link. This multiplier lies in the range $(0,1]$, for the network activities, where $\alpha_a = 1$ means that 100% of the initial flow on link a reaches the successor node of that link, reflecting that there is no decay/waste/loss on link a .

The multiplier α_a can be modeled as the product of two terms, a radioactive decay multiplier α_{d_a} and a processing loss multiplier α_{l_a} .

Radioactive Decay

The activity of a radioisotope (in disintegrations per unit time) is proportional to the quantity of that isotope, i.e.,

$$\frac{dN}{dt} \propto N, \quad (2)$$

where $N = N(t)$ = the quantity of a radioisotope. The quantity of a radioisotope in a time interval t is then given by

$$N(t) = N_0 e^{-\lambda t}, \quad (3)$$

where N_0 is the quantity present at the beginning of the interval and λ is the decay constant of the radioisotope (see Berger, Goldsmith, and Lewis (2004)).

We can represent the radioactive decay multiplier α_{da} for link a as

$$\alpha_{da} = e^{-\lambda t_a}, \quad (4)$$

and t_a is the time spent on link a . The decay constant, λ , in turn, can be conveniently represented by an experimentally measured value, called the half-life $t_{1/2}$, where

$$t_{1/2} = \frac{\ln 2}{\lambda}. \quad (5)$$

The values of the half-lives of radioisotopes are tabulated in the American Institute of Physics (1972). We can write α_{da} as

$$\alpha_{da} = e^{-\lambda t_a} = e^{-\ln 2 \frac{t_a}{t_{1/2}}} = 2^{-\frac{t_a}{t_{1/2}}}. \quad (6)$$

The value of $t_{1/2}$ for Mo is 66.7 hours.

The processing loss multiplier α_{I_a} for link a is a factor in the range $(0,1]$ that quantifies for the losses that occur during processing. Different processing links may have different values for this parameter.

For transportation links there is no loss beyond that due to radioactive decay; therefore, $\alpha_{I_a} = 1$ for such links. For the top-most manufacturing links $\alpha_a = 1$.

Recall that f_a denotes the (initial) flow on link a . Let f'_a denote the final flow on that link; i.e., the flow that reaches the successor node of the link. Therefore,

$$f'_a = \alpha_a f_a, \quad \forall a \in L. \quad (7)$$

The organization is also responsible for disposing the waste which is hazardous.

The Link Discarding Costs

Since α_a is constant, and known a priori, a total discarding cost function, \hat{z}_a , can be defined accordingly, which is a function of the flow, f_a , and is assumed to be convex and continuously differentiable and given by:

$$\hat{z}_a = \hat{z}_a(f_a), \quad \forall a \in L. \quad (8)$$

Note that, in processing/producing an amount of radioisotope f_a , one knows from the physics the amount of hazardous waste and, hence, a discarding function of the form (8) is appropriate.

Let x_p represent the (initial) flow of Mo on path p joining the origin node with a destination node. The path flows must be nonnegative, that is,

$$x_p \geq 0, \quad \forall p \in \mathcal{P}. \quad (9)$$

Let μ_p denote the multiplier corresponding to the loss on path p , which is defined as the product of all link multipliers on links comprising that path, that is,

$$\mu_p \equiv \prod_{a \in p} \alpha_a, \quad \forall p \in \mathcal{P}. \quad (10)$$

The demand at demand point R_k , d_k , is the sum of all the final flows on paths joining $(0, H_k^2)$:

$$d_k \equiv \sum_{p \in \mathcal{P}_{w_k}} \mu_p x_p, \quad k = 1, \dots, n_H. \quad (11)$$

Although the amount of radioisotope that originates on a path p is x_p , the amount (due to radioactive decay, etc.) that actually arrives at the destination (terminal node) of this path is $x_p \mu_p$.

The multiplier α_{ap} is the product of the multipliers of the links on path p that precede link a in that path. This multiplier can be expressed as:

$$\alpha_{ap} \equiv \begin{cases} \delta_{ap} \prod_{a' < a} \alpha_{a'}, & \text{if } \{a' < a\} \neq \emptyset, \\ \delta_{ap}, & \text{if } \{a' < a\} = \emptyset, \end{cases} \quad (12)$$

where $\{a' < a\}$ denotes the set of the links preceding link a in path p , and δ_{ap} is defined as equal to one if link a is contained in path p ; otherwise, it is equal to zero, and \emptyset denotes the null set. In other words, α_{ap} is equal to the product of all link multipliers preceding link a in path p . If link a is not contained in path p , then α_{ap} is set to zero.

The relationship between the link flow, f_a , and the path flows is:

$$f_a = \sum_{p \in \mathcal{P}} x_p \alpha_{ap}, \quad \forall a \in L. \quad (13)$$

The Organization's Objectives

The organization wishes to determine which facilities should operate and at what level, and is also interested in possibly redesigning the existing capacities with the demand being satisfied, and the total cost being minimized.

The Link Investment / Reduction Costs

Let \bar{u}_a denote the nonnegative existing capacity on link a , $\forall a \in L$. The organization can enhance/reduce the capacity of link a by u_a , $\forall a \in L$. The total investment cost of adding capacity u_a on link a , or contrarily, the induced cost of lowering the capacity by u_a , is denoted by $\hat{\pi}_a$, and is a function of the change in capacity:

$$\hat{\pi}_a = \hat{\pi}_a(u_a), \quad \forall a \in L. \quad (14)$$

These functions are also assumed to be convex and continuously differentiable. We group the link capacity changes into the vector u . The path flows and the link flows, in turn, are grouped into the respective vectors: x and f .

The Total Cost Minimization Problem

The total cost minimization objective faced by the organization includes the total cost of operating the various links, the total discarding cost of waste/loss over the links, and the total cost of capacity modification. This optimization problem can be expressed as:

$$\text{Minimize } \sum_{a \in L} \hat{c}_a(f_a) + \sum_{a \in L} \hat{z}_a(f_a) + \sum_{a \in L} \hat{\pi}_a(u_a) \quad (15)$$

subject to: constraints (9), (11), and (13), and

$$f_a \leq \bar{u}_a + u_a, \quad \forall a \in L, \quad (16)$$

$$-\bar{u}_a \leq u_a, \quad \forall a \in L. \quad (17)$$

If $\bar{u}_a = 0, \forall a \in L$, then the redesign model converts to a “design from scratch” model.

The Decision-Making Problems in Link Flows and in Path Flows

The supply chain network design problem for a medical nuclear product can be expressed as a decision-making problem:

$$\text{Minimize } \sum_{a \in L} \hat{c}_a(f_a) + \sum_{a \in L} \hat{z}_a(f_a) + \sum_{a \in L} \hat{\pi}_a(u_a) \quad (18)$$

subject to: constraints: (9), (11), (13), (16), and (17).

The above optimization problem can also be expressed in terms of path flows:

$$\text{Minimize } \sum_{p \in \mathcal{P}} (\hat{C}_p(x) + \hat{Z}_p(x)) + \sum_{a \in L} \hat{\pi}_a(u_a) \quad (19)$$

subject to: constraints (9), (11), (13), (16), and (17),

where the total operational cost, $\hat{C}_p(x)$ and the total discarding cost, $\hat{Z}_p(x)$, corresponding to path p , are, respectively, derived from $C_p(x)$ and $Z_p(x)$ as:

$$\begin{aligned}\hat{C}_p(x) &= x_p \times C_p(x), & \forall p \in \mathcal{P}, \\ \hat{Z}_p(x) &= x_p \times Z_p(x), & \forall p \in \mathcal{P}\end{aligned}\quad (20)$$

with the unit cost functions on path p , i.e., $C_p(x)$ and $Z_p(x)$ defined as:

$$\begin{aligned}C_p(x) &\equiv \sum_{a \in L} c_a(f_a) \alpha_{ap}, & \forall p \in \mathcal{P}, \\ Z_p(x) &\equiv \sum_{a \in L} z_a(f_a) \alpha_{ap}, & \forall p \in \mathcal{P}.\end{aligned}\quad (21)$$

The Feasible Set

We associate the Lagrange multiplier γ_a with constraint (16) for each link a , and we denote the optimal Lagrange multiplier by γ_a^* , $\forall a \in L$ and group them into the vectors γ and γ^* , respectively. Let K denote the feasible set such that:

$$K \equiv \{(x, u, \gamma) \mid x \in R_+^{n_p}, (11) \text{ and } (17) \text{ hold}, \gamma \in R_+^{n_L}\}. \quad (22)$$

A Lemma

Lemma: *The partial derivatives of the total operational cost and the total discarding cost with respect to a path flow are, respectively, given by:*

$$\begin{aligned}\frac{\partial(\sum_{q \in \mathcal{P}} \hat{C}_q(x))}{\partial x_p} &\equiv \sum_{a \in L} \frac{\partial \hat{c}_a(f_a)}{\partial f_a} \alpha_{ap}, \quad \forall p \in \mathcal{P}, \\ \frac{\partial(\sum_{q \in \mathcal{P}} \hat{Z}_q(x))}{\partial x_p} &\equiv \sum_{a \in L} \frac{\partial \hat{z}_a(f_a)}{\partial f_a} \alpha_{ap}, \quad \forall p \in \mathcal{P},\end{aligned}\quad (23)$$

Proof: See Nagurney, Masoumi, and Yu (2010) for the proof.

A Theorem

Theorem: Variational Inequality Formulations: *The optimization problem (19), subject to its constraints, is equivalent to the variational inequality problem: determine the vector of optimal path flows, the vector of optimal capacity adjustments, and the vector of optimal Lagrange multipliers $(x^*, u^*, \gamma^*) \in K$, such that:*

$$\begin{aligned} & \sum_{k=1}^{nR} \sum_{p \in \mathcal{P}_{w_k}} \left[\frac{\partial(\sum_{q \in \mathcal{P}} \hat{C}_q(x^*))}{\partial x_p} + \frac{\partial(\sum_{q \in \mathcal{P}} \hat{Z}_q(x^*))}{\partial x_p} + \sum_{a \in L} \gamma_a^* \delta_{ap} \right] \\ & \quad \times [x_p - x_p^*] + \sum_{a \in L} \left[\frac{\partial \hat{\pi}_a(u_a^*)}{\partial u_a} - \gamma_a^* \right] \times [u_a - u_a^*] \\ & + \sum_{a \in L} \left[\bar{u}_a + u_a^* - \sum_{p \in \mathcal{P}} x_p^* \alpha_{ap} \right] \times [\gamma_a - \gamma_a^*] \geq 0, \forall (x, u, \gamma) \in K. \quad (24) \end{aligned}$$

Variational inequality (24), in turn, can be rewritten in terms of link flows as: determine the vector of optimal link flows, the vector of the link capacity adjustments, and the vector of optimal Lagrange multipliers $(f^*, u^*, \gamma^*) \in K^1$, such that:

$$\begin{aligned} & \sum_{a \in L} \left[\frac{\partial \hat{c}_a(f_a^*)}{\partial f_a} + \frac{\partial \hat{z}_a(f_a^*)}{\partial f_a} + \gamma_a^* \right] \times [f_a - f_a^*] \\ & + \sum_{a \in L} \left[\frac{\partial \hat{\pi}_a(u_a^*)}{\partial u_a} - \gamma_a^* \right] \times [u_a - u_a^*] \\ & + \sum_{a \in L} [\bar{u}_a + u_a^* - f_a^*] \times [\gamma_a - \gamma_a^*] \geq 0, \quad \forall (f, u, \gamma) \in K^1, \quad (25) \end{aligned}$$

where K^1 denotes the feasible set:

$$K^1 \equiv \{(f, u, \gamma) | \exists x \geq 0, (9), (11), (13), (17) \text{ hold, and } \gamma \geq 0\}. \quad (26)$$

Variational inequality (24) can be put into standard form VI (F, \mathcal{K}) (see Nagurney (1999)) as follows: determine $X^* \in \mathcal{K}$ such that:

$$\langle F(X^*)^T, X - X^* \rangle \geq 0, \quad \forall X \in \mathcal{K}. \quad (27)$$

The Computational Approach

The Computational Approach

We propose the modified projection method for the VI in path flows, rather than in link flows, since, in the context of our new model, it yields subproblems that can be solved exactly, and in closed form, using a variant of the exact equilibration algorithm, adapted to incorporation of arc/path multipliers, along with explicit formulae for the capacity investments, and the Lagrange multipliers.

It is guaranteed to converge if the function F that enters the variational inequality satisfies monotonicity and Lipschitz continuity (see Korpelevich (1977) and Nagurney (1999)).

The Modified Projection Method

We now recall the modified projection method, where \mathcal{T} denotes an iteration counter.

Step 0: Initialization

Set $X^0 \in \mathcal{K}$. Let $\mathcal{T} = 1$ and let η be a scalar such that $0 < \eta \leq \frac{1}{L}$, where L is the Lipschitz continuity constant.

Step 1: Computation

Compute $\tilde{X}^{\mathcal{T}}$ by solving the VI subproblem:

$$\langle \tilde{X}^{\mathcal{T}} + \eta F(X^{\mathcal{T}-1}) - X^{\mathcal{T}-1}, X - \tilde{X}^{\mathcal{T}} \rangle \geq 0, \quad \forall X \in \mathcal{K}. \quad (28)$$

Step 2: Adaptation

Compute $X^{\mathcal{T}}$ by solving the VI subproblem:

$$\langle X^{\mathcal{T}} + \eta F(\tilde{X}^{\mathcal{T}}) - X^{\mathcal{T}-1}, X - X^{\mathcal{T}} \rangle \geq 0, \quad \forall X \in \mathcal{K}. \quad (29)$$

Step 3: Convergence Verification

If $\max |X_l^{\mathcal{T}} - X_l^{\mathcal{T}-1}| \leq \epsilon$, for all l , with $\epsilon > 0$, a prespecified tolerance, then stop; else, set $\mathcal{T} =: \mathcal{T} + 1$, and go to Step 1.

Explicit Formulae for the Investment Capacities and Lagrange Multipliers

The VI subproblems in (28) and (29) are quadratic programming problems with special structure that result in straightforward computations. Explicit formulae for (28) for the supply chain network design problem are now given for the capacity investments and the Lagrange multipliers. Analogous formulae for (29) can then be easily obtained.

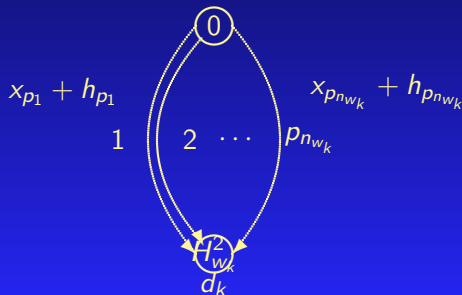
Explicit Formulae for the Investment Capacities and the Lagrange Multipliers at Step 1 (cf. (28))

$$\tilde{u}_a^T = \max\left\{-\bar{u}_a, u_a^{T-1} + \eta\left(\gamma_a^{T-1} - \frac{\partial \hat{\pi}_a(u_a^{T-1})}{\partial u_a}\right)\right\}, \quad \forall a \in L; \quad (30)$$

$$\tilde{\gamma}_a^T = \max\left\{0, \gamma_a^{T-1} + \eta\left(\sum_{p \in \mathcal{P}} x_p^{T-1} \alpha_{ap} - u_a^{T-1} - \bar{u}_a\right)\right\}, \quad \forall a \in L. \quad (31)$$

Exploitation of Special Network Structure for Path Flow Subproblems via Exact Equilibration

Recall that the feasible set \mathcal{K} , in terms of the path flows, requires that the path flows be nonnegative and that the demand constraint (11) holds for each demand point. The induced path flow subproblems in (28) and (29), hence, have a special network structure of the form given in Figure 2 below.



The path flow subproblems that one must solve in Step 1 (see (28)) (we have suppressed the iteration superscripts below) have the following form for each demand point k ; $k = 1, \dots, n_H$:

$$\text{Minimize } \frac{1}{2} \sum_{p \in \mathcal{P}_{w_k}} x_p^2 + \sum_{p \in \mathcal{P}_{w_k}} h_p x_p$$

subject to:

$$d_k \equiv \sum_{p \in \mathcal{P}_{w_k}} \mu_p x_p,$$

$$x_p \geq 0, \quad \forall p \in \mathcal{P}_{w_k},$$

where

$$h_p \equiv x_p^{T-1} - \eta \left[\frac{\partial(\sum_{q \in \mathcal{P}} \hat{C}_q(x^{T-1}))}{\partial x_p} + \frac{\partial(\sum_{q \in \mathcal{P}} \hat{Z}_q(x^{T-1}))}{\partial x_p} + \sum_{a \in L} \gamma_a^{T-1} \delta_{ap} \right].$$

An Exact Equilibration Algorithm

Step 0: Sort

Sort the fixed terms h_p ; $p \in \mathcal{P}_{w_k}$ in nondescending order and relabel the paths/links accordingly. Assume that they are relabeled. Set $h_{p_{n_{w_k}+1}} \equiv \infty$, where n_{w_k} denotes the number of paths connecting destination node H_k^2 with origin node 0. Set $r = 1$.

Step 1: Computation

Compute

$$\lambda_k^r = \frac{\sum_{i=1}^r \mu_{p_i} h_{p_i} + d_k}{\sum_{i=1}^r \mu_{p_i}^2}.$$

Step 2: Evaluation

If $h_{p_r} < \lambda_k^r \leq h_{p_{r+1}}$, then stop; set $s = r$ and go to Step 3; otherwise, let $r = r + 1$ and return to Step 1.

Step 3: Path Flow Determination

Set

$$x_{p_i} = \mu_{p_i} \lambda_k^s - h_{p_i}, \quad i = 1, \dots, s.$$
$$x_{p_i} = 0, \quad i = s + 1, \dots, n_{w_k}.$$

Highlights of a Case Study

Highlights of a Case Study

In our paper, we considered the Molybdenum-99 supply chain in North America with the focus on the Canadian reactor, the Canadian processing facility, and the two US generator manufacturing facilities.

This reactor is to be decommissioned around 2016; the same holds for the processing facility.

Highlights of a Case Study

The reactor, known as NRU, is located in Chalk River, Ontario.

The processing facility is located in Ottawa, and is known as AECL-MDS Nordion.

Transportation of the irradiated targets from NRU to AECL - MDS Nordion takes place by truck.

There are two generator manufacturers in the United States (and none in Canada). The two existing generator manufacturers are located in Billerica, Massachusetts and outside of St. Louis, Missouri.

We considered the supply chain network design problem from scratch. Hence, we assumed that the $\bar{u}_a = 0.00$, for all links a .

Highlights of a Case Study

We implemented the modified projection method, along with the generalized exact equilibration algorithm for the solution of our supply chain network design problem. The ϵ in the convergence criterion was 10^{-6} . The algorithm was implemented in FORTRAN and a Unix-based system at the University of Massachusetts was used for the computations.

Highlights of a Case Study

We calculated the values of the arc multipliers α_{da} , for all links $a = 1, \dots, 20$, using data in the OECD (2010a) report and in the National Research Council (2009) report, which included the approximate times associated with the various links in the supply chain network in Figure 3. According to OECD (2010a), we may assume that there is no loss α_{la} on each link a for $a = 1, \dots, 20$, except for processing link 3; hence, $\alpha_{la} = 1$ for all the former links; therefore, $\alpha_a = \alpha_{da}$ for all those links, as reported in Table 1. In the case of link 3, $\alpha_{la} = .8$ and $\alpha_{da} = .883$; therefore, $\alpha_3 = .706$. All capacities and flows are reported in Curies.

Highlights of a Case Study

Capital and operating cost data were taken from OECD (2010b) and converted to per Curie processed or generated. As noted by the National Research Council (2009), the US generator prices are proprietary, but could be estimated from a functional form derived from publicly available prices for Australian generators coupled with several spot prices for US made generators.

We assumed three demand points corresponding, respectively, to the collective demands in the US, in Canada, and in other countries (such as Mexico, and the Caribbean Islands). We are using 3 demand points, as approximations, in order to be able to report the input and output data for transparency purposes. The demands were as follows: $d_1 = 3,600$, $d_2 = 1,800$, and $d_3 = 1,000$ and these denote the demands, in Curies, per week. These values were obtained by using the daily number of procedures in the US and extrapolating for the others. The unites for the path and link flows are also Curies.

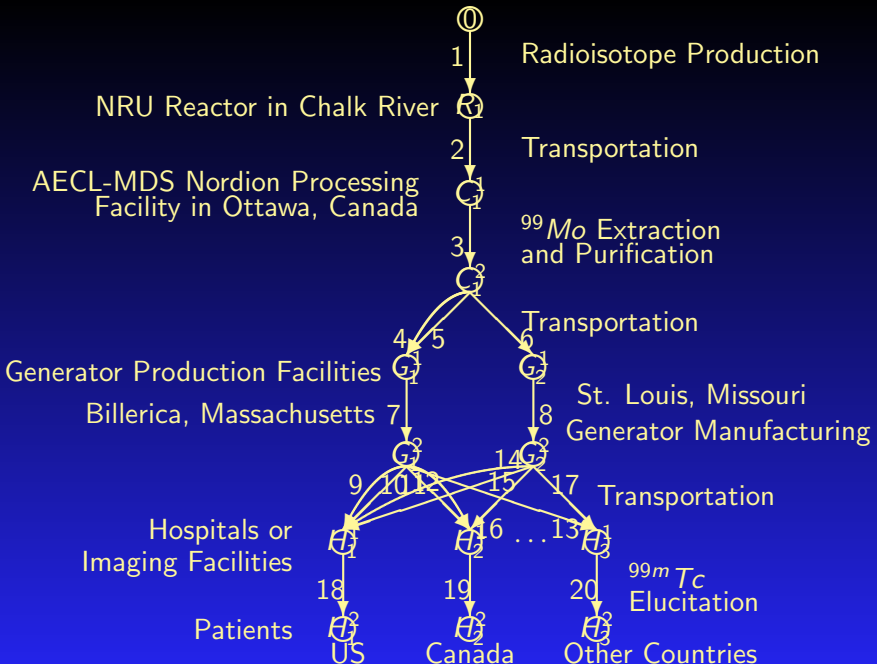


Figure 3: The Existing Supply Chain Topology

Table 1: Input Data and Optimal Link Flow and Capacity Solution

Link a	α_a	$\hat{c}_a(f_a)$	$\hat{z}_a(f_a)$	$\hat{\pi}_a(u_a)$	\bar{u}_a	f_a^*	u_a^*
1	1.00	$2f_1^2 + 25.6f_1$	0.00	$u_1^2 + 743u_1$	0.00	15,034	15,034
2	.969	$f_2^2 + 5f_2$	0.00	$.5u_2^2 + u_2$	0.00	15,034	15,034
3	.706	$5f_3^2 + 192f_3$	$5f_3^2 + 80f_3$	$.5u_3^2 + 289u_3$	0.00	14,568	14,568
4	.920	$2f_4^2 + 4f_4$	0.00	$.5u_4^2 + 4u_4$	0.00	4,254	4,253
5	.901	$f_5^2 + f_5$	0.00	$2.5u_5^2 + 2u_5$	0.00	1,286	1,286
6	.915	$f_6^2 + 2f_6$	0.00	$.5u_6^2 + u_6$	0.00	4,744	4,744
7	.804	$f_7^2 + 166f_7$	$2f_7^2 + 7f_7$	$.5u_7^2 + 289u_7$	0.00	5,072	5,072
8	.804	$f_8^2 + 166f_8$	$2f_7^2 + 7f_7$	$.5u_8^2 + 279u_8$	0.00	4,341	4,341
9	.779	$2f_9^2 + 4f_9$	0.00	$.5u_9^2 + 3u_9$	0.00	0.00	0.00
10	.883	$f_{10}^2 + 1f_{10}$	0.00	$.5u_{10}^2 + 5u_{10}$	0.00	2,039	2,039
11	.883	$2f_{11}^2 + 4f_{11}$	0.00	$.5u_{11}^2 + 3u_{11}$	0.00	2,039	2,039
12	.688	$f_{12}^2 + 2f_{12}$	0.00	$.5u_{12}^2 + f_{12}$	0.00	0.00	0.00
13	.688	$2.5f_{13}^2 + 2f_{13}$	0.00	$.5f_{13}^2 + u_{13}$	0.00	0.00	0.00
14	.779	$2f_{14}^2 + 2f_{14}$	0.00	$u_{14}^2 + uf_{14}$	0.00	0.00	0.00
15	.883	$f_{15}^2 + 7f_{15}$	0.00	$2u_{15}^2 + 5u_{15}$	0.00	2,037	2,037
16	.688	$2f_{16}^2 + 4f_{16}$	0.00	$.5u_{16}^2 + u_{16}$	0.00	0.00	0.00
17	.688	$2f_{17}^2 + 6f_{17}$	0.00	$u_{17}^2 + u_{17}$	0.00	1,453	1,453
18	1.00	$2f_{18}^2 + 800f_{18}$	$4f_{18}^2 + 80f_{18}$	$.5u_{18}^2 + 10u_{18}$	0.00	3,600	3,600
19	1.00	$f_{19}^2 + 600f_{19}$	$1f_{19}^2 + 60f_{19}$	$.5u_{19}^2 + 5u_{19}$	0.00	1,800	1,800
20	1.00	$f_{20}^2 + 300f_{20}$	$1f_{20}^2 + 30f_{20}$	$.5u_{20}^2 + 2u_{20}$	0.00	1,000	1,000

Highlights of a Case Study

The total cost associated with this supply chain network design was: 2,976,125,952.00.

The computed capacity at the Canadian reactor is 33,535, whereas the computed capacity at the processor is 32,154. Hence, one can infer from the above analysis that both of these are operating with excess capacity, which has been noted in the literature.

The case study demonstrates how data can be acquired and the relevance of the output results. With our model, a cognizant organization can then investigate the costs associated with new supply chain networks for a radioisotope used in medical imaging and diagnostics.

Summary and Suggestions for Future Research

Summary and Suggestions for Future Research

In this paper, we developed a rigorous framework for the design and redesign of medical nuclear supply chains.

We focused on the most widely used radioisotope, Molybdenum, ^{99}Mo , which is used in medical diagnostics for cancer and cardiac problems. *Nuclear supply chains have numerous challenging features, including: time-sensitivity of the product, which is subject to radioactive decay, the hazardous nature of production and transportation as well as waste disposal.*

Radioisotopes are produced globally in only a handful of reactors and the same holds for their processing.

The nuclear reactors where they are produced are aging and have been subject to failures creating shortages of this critical healthcare product.

The specific contributions of the findings in this paper are:

- (1). a theoretically sound, based on physics principles, methodology to determine the flow of the radioisotope on various processing links of the supply chain network, through the use of arc multipliers;
- (2). a generalized network, decision-making system optimization model that includes the relevant criteria associated with link expansion/reduction, coupled with the operational costs and the associated discarding and waste management costs, subject to demand satisfaction;
- (3). a unified framework that can handle either design of the network from scratch or a redesign, with specific relevance to the existing economic and engineering situation, coupled with the physics underlying the time-decay of the radioisotope, and
- (4). an algorithm which resolves the supply chain network design problem into subproblems with elegant features for computation.

The contributions in the paper can serve as *foundation for the investigation of other medical nuclear product supply chains.*

The framework can serve as the basis for *exploration of alternative behaviors among the various stakeholders, including competition.*

It can be used to *the vulnerability of medical nuclear supply chains* and to explore alternative topologies and the associated costs.

THANK YOU!



The Virtual Center for Supernetworks



Supernetworks for Optimal Decision-Making and Improving the Global Quality of Life

[Home](#) [About](#) [Background](#) [Activities](#) [Publications](#) [Media](#) [Links](#) [What's New](#) [Search](#)



Professor Nagurney receives the Jane F. Garvey Award

The Virtual Center for Supernetworks at the Isenberg School of Management, under the directorship of Anna Nagurney, the John F. Smith Memorial Professor, is an interdisciplinary center, and includes the Supernetworks Laboratory for Computation and Visualization.

Mission: The mission of the Virtual Center for Supernetworks is to foster the study and application of supernetworks and to serve as a resource to academia, industry, and government on networks ranging from transportation, supply chains, telecommunication, and electric power networks to economic, environmental, financial, knowledge and social networks.

The Applications of Supernetworks Include: multimodal transportation networks, critical infrastructure, energy and the environment, the Internet and electronic commerce, global supply chain management, international financial networks, web-based advertising, complex networks and decision-making, integrated social and economic networks, network games, and network metrics.

Announcements and Notes from the Center Director
Professor Anna Nagurney

Updated: April 8, 2011

Professor Anna Nagurney's Blog

RENEW

Research, Education, Networks, and the World: A Female Professor Speaks

INFORMS Podcasts: Anna Nagurney on Supernetworks

Why did closing New York's Tappan Zee Bridge to cars improve traffic? How are energy and finance like large networks? Can biologists learn from operations researchers? Anna Nagurney, Director of the Virtual Center for Supernetworks at the Isenberg School of Management, is featured in the latest INFORMS podcast. Tune in at www.informs.org/podcasts



Photos of Center Activities



The Braess Paradox Translation Information Photos



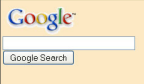
You are visitor number

69,032

to the Virtual Center for Supernetworks.



Humanitarian Logistics: Networks for Africa



For more information, see: <http://supernet.isenberg.umass.edu>